

Full stabilization of eight-channel Yb-fiber coherent beam combining system delivering 1.18-kW, 1.18-mJ, 270-fs pulses

Zhuo Shi(史卓), Zhi-Hang Du(杜志航), Cheng-Bin Liang(梁成斌), Hong-Xiang Chang(常洪祥), Zi-Kai Dong(董自凯), Hong-Yu Guo(郭鸿宇), Can Li(李灿), Pu Zhou(周朴), Zhi-Yi Wei(魏志义), and Guo-Qing Chang(常国庆)
Citation: Chin. Phys. B, 2026, 35 (**2**): 024210. DOI: 10.1088/1674-1056/ae1952
http://cpb.iphy.ac.cn; http://iopscience.iop.org/cpb

What follows is a list of articles you may be interested in

Tea polyphenol polymer film enables broadband optical modulation for hybrid mode-locked ultrafast fiber lasers

Wei Chen(陈伟), Kang Li(李康), Cheng Gao(高成), Qingping Hu(胡庆平), Zhengfan Li(黎征帆), Yi Xiong(熊祎), and Yunzhou Sun(孙运周)
Chin. Phys. B, 2026, 35 (**2**): 024209. DOI: 10.1088/1674-1056/ae156e

Optomechanical-organized multipulse dynamics in ultrafast fiber laser

Lin Huang(黄琳), Yu-Sheng Zhang(张裕生), and Yu-Dong Cui(崔玉栋)
Chin. Phys. B, 2021, 30 (**11**): 114203. DOI: 10.1088/1674-1056/abf344

Self-starting all-fiber PM Er: laser mode locked by a biased nonlinear amplifying loop mirror

Ke Yin(殷科), Yi-Ming Li(李仪茗), Yan-Bin Wang(王彦斌), Xin Zheng(郑鑫), Tian Jiang(江天)
Chin. Phys. B, 2019, 28 (**12**): 124203. DOI: 10.1088/1674-1056/ab4d42

Two-dimensional materials-decorated microfiber devices for pulse generation and shaping in fiber lasers

Zhi-Chao Luo(罗智超), Meng Liu(刘萌), Ai-Ping Luo(罗爱平), Wen-Cheng Xu(徐文成)
Chin. Phys. B, 2018, 27 (**9**): 094215. DOI: 10.1088/1674-1056/27/9/094215

Sb_2Te_3 mode-locked ultrafast fiber laser at 1.93 μm

Jintao Wang(王金涛), Jinde Yin(尹金德), Tingchao He(贺廷超), Peiguang Yan(闫培光)
Chin. Phys. B, 2018, 27 (**8**): 084214. DOI: 10.1088/1674-1056/27/8/084214

INSTRUMENTATION AND MEASUREMENT

Full stabilization of eight-channel Yb-fiber coherent beam combining system delivering 1.18-kW, 1.18-mJ, 270-fs pulses

Zhuo Shi(史卓)[1,2], Zhi-Hang Du(杜志航)[2], Cheng-Bin Liang(梁成斌)[2], Hong-Xiang Chang(常洪祥)[3], Zi-Kai Dong(董自凯)[2], Hong-Yu Guo(郭鸿宇)[2], Can Li(李灿)[3], Pu Zhou(周朴)[3], Zhi-Yi Wei(魏志义)[1,2,4], and Guo-Qing Chang(常国庆)[1,2,4,†]

[1] *Beijing National Laboratory for Condensed Matter Physics, Institute of Physics, Chinese Academy of Sciences, Beijing* 100190, *China*
[2] *Songshan Lake Materials Laboratory, Dongguan* 523808, *China*
[3] *College of Advanced Interdisciplinary Studies, National University of Defense Technology, Changsha* 410073, *China*
[4] *University of Chinese Academy of Sciences, Beijing* 100049, *China*

(Received 9 September 2025; revised manuscript received 16 October 2025; accepted manuscript online 30 October 2025)

We develop an ultrafast Yb-fiber laser system based on eight-channel coherent beam combining utilizing commercially available rod-type Yb-fibers. To ensure good combining efficiency and long-term operation of the system at the attosecond laser facility under construction, we fully stabilize the phase, group-delay, and beam-pointing of the eight fiber channels. Especially, we propose a novel multi-step hill climbing method to control both group-delay and beam-pointing. At a repetition rate of 1 MHz, this laser system delivers 270-fs pulses with 1.18-kW average power (1.18-mJ pulse energy). The average-power instability of the laser system running for 12 hours is 0.32%.

Keywords: ultrafast fiber laser, high power and high energy, coherent beam combining

PACS: 42.55.Wd, 42.60.–v, 42.81.–i

DOI: 10.1088/1674-1056/ae1952 **CSTR:** 32038.14.CPB.ae1952

1. Introduction

At present, several countries around the world are actively constructing large-scale attosecond laser facilities, such as Attosecond Light Pulse Source (ALPS) in Europe, Synergetic Extreme Condition User Facility (SECUF) in China, and National eXtreme Ultrafast Science (NeXUS) facility in USA.[1–3] An advanced attosecond laser facility is under construction in Dongguan, China, which includes six beamlines. One of the beamlines is designed to produce high photon-flux extreme ultraviolet pulses via high-order harmonic generation. To meet the design parameters, this beamline demands femtosecond driving pulses centered at 1.03 μm with $>$ 1-kW average power and $>$ 1-mJ pulse energy. These powerful and energetic pulses can be obtained by using coherent beam combining (CBC) of multiple Yb-fiber chirped-pulse amplifiers. In 2020, Müller *et al.* implemented a twelve-channel CBC Yb-fiber laser system with an average power as high as 10.4 kW despite the relatively low pulse energy of 130 μJ.[4] In 2023, Stark *et al.* developed a sixteen-channel CBC system incorporating temporal pulse division, which generated 32-mJ, 158-fs pulses with an average power of 703 W.[5]

In a CBC fiber-laser system, one pulse is spatially split into several replicas, then amplified in multiple fiber amplifiers, and finally combined into one pulse to overcome the limitation of single fiber amplifiers. Implementation of CBC requires active phase stabilization in order to ensure that all pulse replicas maintain the identical phase and thus reach a high combining efficiency; meanwhile, stabilization of relative group-delay and beam-pointing among pulse replicas is demanded for long-term operation. To produce femtosecond pulses with $>$ 1-mJ energy, fiber-laser CBC systems normally utilize rod-type Yb-fibers as the gain media. These fibers have mode areas 100 times larger than conventional single-mode fibers while maintaining quasi single-mode output.[6] Recently, NKT company has developed a new version of rod-type Yb-fiber specially designed to suppress transverse-mode instability (TMI), which limits the average power scaling in fiber lasers.[7,8] In 2024, we obtained 323-W output power from a single amplifier based on this rod-type Yb-fiber seeded with 30-W input power.[9] Given the superior power scalability, this new rod-type fiber is well suited for constructing a high-power CBC system. In 2025, we demonstrated a four-channel CBC system that delivered a maximum average power of 753-W and a maximum pulse energy of 1.07-mJ;[10] Wang *et al.* constructed a six-channel CBC system producing femtosecond pulses with 1.2-kW average power and 1.2-mJ pulse energy.[11] Unfortunately, both of these CBC systems only implemented phase stabilization. However, lack of group-delay and beam-pointing stabilization made these CBC systems vulnerable to thermal and environmental disturbance. Consequently, they cannot be used for practical applications (e.g.,

†Corresponding author. E-mail: guoqing.chang@iphy.ac.cn

© 2026 Chinese Physical Society and IOP Publishing Ltd. All rights, including for text and data mining, AI training, and similar technologies, are reserved.

serving as the driving source of attosecond laser beamlines) that demand long-term stable operation.

To date, most of the reported high-power Yb-fiber CBC systems rely on Hänsch–Couillaud (HC) polarization detection or the locking of optical coherence by the single-detector electronic frequency-tagging (LOCSET) method for active phase stabilization.[12,13] HC features simple signal processing logic, large bandwidth, and small phase residual error. However, the high complexity of combining structure and electronic devices limits the channel scaling of HC-based CBC, which increases even more when group-delay and beam-pointing control is involved. LOCSET uses modulation and demodulation processes to achieve phase stabilization with a simplified combining structure, but each channel needs a unique modulation frequency, which prevents the channel scaling of LOCSET-based CBC due to the limited bandwidth of the phase controller. In contrast, a hill-climbing method called stochastic parallel gradient descent (SPGD) has simple signal process logic, and needs only one photodetector (PD) for phase stabilization of any number of channels, which exhibits good stability and reliability when the number of channels reaches more than 100, making it an ideal method for CBC with large channel number.[14] Among all three methods mentioned above, the HC method offers the fastest calculation speed, followed by LOCSET, with SPGD being the slowest. However, SPGD excels in structural simplicity, and the convergence for a small number of combining channels is fast enough to maintain excellent stability and high combining efficiency.

In this paper, we develop an eight-channel CBC laser system based on NKT TMI-suppressed rod-type Yb-fibers. Besides achieving phase stabilization by SPGD, we demonstrate a novel multi-step hill-climbing method utilizing uncombined outputs to control group-delay and beam-pointing. By the compensation of high-order dispersion between programmable chirped fiber Bragg grating (CFBG) and grating pair compressor, our CBC system delivers 1.18-mJ, 270-fs pulses with an average power of 1.18 kW. The phase residual error is $\lambda/29.5$, and the root-mean-square (RMS) of average-power is 0.32% in a 12-hour measurement.

2. Experimental setup

Figure 1 illustrates our experimental setup consisting of five stages: frontend, beam splitting stage, main amplifiers, beam combining stage, and compressor.

The frontend includes a Yb-fiber oscillator, a stretcher, a pulse picker and three pre-amplifiers. The pulses emitted by the 45-MHz oscillator center at 1033 nm with a spectral width of 16 nm. These seeding pulses are stretched to about 1 ns by a stretcher made of two cascaded CFBGs with total group-delay dispersion of 38.7 ps^2. The third-, fourth-, and fifth-order dispersions can be tuned by thermoelectric coolers attached to both CFBGs. Afterward, the first pre-amplifier based on polarization maintaining Yb-doped fiber increases the average power to 300 mW, and an acousto-optic modulator serving as pulse picker then reduces the pulse repetition-rate from 45 MHz to 1 MHz. Finally, the second and third pre-amplifiers increase the average power of pulses to 50 mW and 40 W, respectively. The second pre-amplifier is similar to the first one, and the third pre-amplifier is constructed using a rod-type Yb-fiber configured at dual-pass. In this configuration, the pulses undergo two amplification passes with the aid of a high-reflection mirror, while their polarization state is rotated between these two passes by a Faraday rotator and a HWP. A pair of lenses are placed between two passes to minimize the beam divergence. The lenses in the telescope have focal lengths of −50 mm and 150 mm, respectively. Such a dual-pass amplifier ensures efficient extraction of pump power leading to a much larger gain compared with the single-pass configuration. At the output of the third pre-amplifiers, the spectral width of pulses is reduced to about 10 nm, and the pulse duration is around 700 ps.

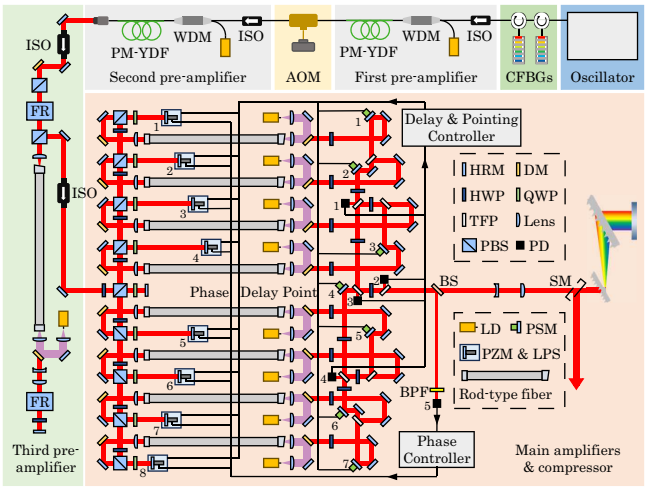


Fig. 1. Schematic setup of the eight-channel coherent beam combining system. CFBG: chirped fiber Bragg grating, ISO: isolator, WDM: wavelength division multiplexer, PM-YDF: polarization maintaining Yb-doped fiber, AOM: acousto-optical modulator, FR: Faraday rotator, HRM: high-reflection mirror, DM: dichroic mirror, HWP: half-wave plate, QWP: quarter-wave plate, TFP: thin-film polarizer, PBS: polarizing beam splitter, PD: photodetector, LD: laser diode, PSM: piezo-steering mirror, PZM: piezo mirror, LPS: linear piezo stage, BS: beam splitter, BPF: band pass filter, SM: square mirror.

The frontend output is spatially split into eight replicas (5-W average power per replica) by a combination of half-wave plates (HWPs) and polarizing beam splitters (PBSs). After passing through delay lines made up of quarter-wave plates (QWPs), piezo mirrors (PZMs) and linear piezo stages (LPSs), the pulse replicas are coupled into eight main amplifiers. The travelling ranges of PZM and LPS are 3 μm and 10 mm, respectively. Each main amplifier uses a commercially available (NKT aeroGAIN-ROD 3.1) rod-type Yb-fiber as the gain medium, which is 80-cm long with a core diameter of 85 μm

(mode-field diameter of 65 μm). This rod-type fiber is specially designed to suppress TMI, capable of generating average power higher than 300 W.[9] The pump laser diode of each main amplifier centers at 976 nm with a maximum output power of 500 W.

The beam combining stage includes HWPs, thin-film polarizers (TFPs), high-reflection mirrors (HRMs), and piezo steering mirrors (PSMs). In Fig. 1, amplifier channels, LPSs, PSMs, and PDs are numbered in order from top to bottom. The amplified pulse replicas undergo three-stage pairwise combination: eight replicas are combined to four, four replicas to two, and finally two replicas to a single pulse. There are four uncombined outputs in the combining stage, and small portions of them are split by beam splitters (BSs) not shown in Fig. 1 and collected by PDs numbered by 1, 2, 3 and 4. The optical paths of all pulse replicas in the beam combining stage are set to be nearly the same to avoid the decline of combining efficiency caused by beam divergence, while the path difference introduced in the beam splitting stage is compensated by delay lines.

A small part of the combined pulses is separated by a BS, spectrally filtered by a bandpass filter (BPF) with 3-nm bandwidth and collected by the fifth PD (numbered by 5 in Fig. 1) for phase stabilization. The electrical signal of PD5 is processed using SPGD method by a phase controller based on field programmable gate array (FPGA), and the processed signal is then fed back to eight PZMs. An FPGA consists of an array of programmable logic blocks and a hierarchy of reconfigurable interconnects that can be wired together to implement complex digital circuit. In SPGD method, independent random perturbations (δu) are simultaneously applied to all PZMs during each iteration. This yields the corresponding change in the signal of PD5 (δJ). For independent random variables, the mathematical expectation of their product equals the product of their individual mathematical expectations. When the mathematical expectation of each random perturbation is zero, the expectation of the product of these random variables exhibits orthogonality. By multiplying δu and δJ, the gradient of the objective function (signal of PD5) with respect to each independent variable (voltages applied to PZMs) can be isolated, thereby enabling parameter updates. The iteration formula is

$$U_{n+1} = U_n + G\frac{\delta J \delta u}{\sigma^2}, \tag{1}$$

where $U_n = (u_1 u_2, \ldots, u_8)$ is the current voltages applied to PZMs, and U_{n+1} is the voltages in the next step. G is the gain coefficient, and σ^2 is the variance of random perturbations. The configuration of parameter G and σ^2 is contingent on the performance of the PD5 signal. The signal stability critically depends on these parameters remaining within a defined range.

SPGD method only requires one detector and one controller, in which the voltages of all PZMs are taken as independent variables, and the PD signal is taken as the objective function. The gradient of the PD signal is solved by adding independent random perturbation to the voltage of all PZMs such that the combined output power can be maintained at the maximum value through continuous iteration.

Apart from phase stabilization, it is also essential for CBC to actively compensate the long-term drift of group-delay and beam-pointing, especially when the CBC channel number exceeds four. This is because all channels have long-term drift of group-delay and beam-pointing in different directions. As the channel number increases, the total drift grows accordingly and leads to a more adverse effect on the system performance. Different from current group-delay and beam-pointing control methods based on spectral and spatial filtering,[15,16] we propose a novel multi-step hill-climbing method employing the electrical signals generated by PD1–PD4. The three-stage pairwise combination mentioned above can be further divided into seven steps. More specific, signals from PD1 and PD4 correspond to the combination of eight replicas into four, while signals from PD3 (PD2) corresponds to the combination of four (two) to two (one). The mismatch of group-delay and beam-pointing in each step increases the signal of corresponding PD. In each iteration, the control of group-delay and beam-pointing can be divided into seven consecutive steps shown in Table 1. We use basic hill climbing method to minimize PD signal since there is only one independent variable (voltage applied to LPS or PSM) and one objective function (PD signal) in each step. This control process follows the gradient descent principle. First, a fixed small perturbation (Δu) is applied to the controlled devices, and the resulting change in the PD signal (ΔJ) is measured. The ratio between ΔJ and Δu provides an estimate of the PD-signal gradient. Ultimately, by adjusting the devices along the negative gradient direction, the system iteratively approaches the optimal operating point that minimizes the PD signal. The group-delay and beam-pointing are alternately controlled to compensate the long-term drift of the CBC system.

Table 1. Control process of group-delay and beam-pointing

Step	Signal source	Devices under control	Combining channels
1	PD1	LPS1 or PSM1	1,2
2	PD1	LPS3 or PSM3	3,4
3	PD4	LPS5 or PSM5	5,6
4	PD4	LPS7 or PSM7	7,8
5	PD3	LPS1,2 or PSM2	1,2,3,4
6	PD3	LPS5,6 or PSM6	5,6,7,8
7	PD2	LPS1,2,3,4 or PSM4	all

After passing through a pair of lenses as a telescope, the combined pulses (with 6-mm beam diameter) are compressed by a pair of diffraction gratings (line density of 1739 lines/mm). The lenses in the telescope have focal lengths of −200 mm and 300 mm, respectively. The telescope is used

to minimize the beam divergence. As the nonlinear phase accumulated during amplification and the high-order dispersion introduced in the compressor can be finely compensated by the dispersion-tunable CFBGs, our CBC laser system can deliver nearly transform-limited femtosecond pulses.

3. Results and discussion

The black, blue, and red curves in Fig. 2(a) illustrate the total output power, combined power and compressed power as a function of the total pump power. The output power of each main amplifier is nearly the same, and all of them increase linearly with the increasing pump power; the slope efficiency exceeds 50%. As we increase the pump power from 0.21 kW to 2.86 kW, the total output power varies from 0.16 kW to 1.47 kW, and the combined power varies from 0.15 kW to 1.31 kW.

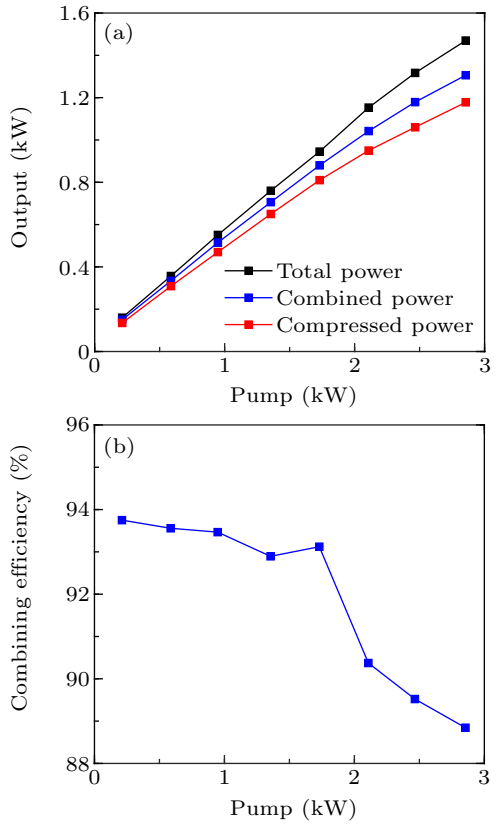


Fig. 2. (a) Total (black), combined (blue) and compressed (red) power versus pump power. (b) Combining efficiency versus pump power.

The blue curve in Fig. 2(b) illustrates the combining efficiency as a function of the total pump power. The combining efficiency is maintained above 93% under low-power conditions. When the total pump power exceeds 2 kW, the nonlinearity and thermal effects become significant, and, therefore, the difference between main amplifiers gradually decreases the combining efficiency to 89%. More specifically, the gain-coefficient difference between the eight channels imposes different nonlinear phase shifts on the pulse replicas through self-phase modulation and Kramers–Krönig coupling, which causes the drop of combining efficiency at high power level. Meanwhile, the heat dissipation differs among eight channels and results in different fiber core temperatures; as the pump power exceeds 2 kW, this temperature difference introduces noticeable variation among beam profiles, which decreases the combining efficiency as well. The maximum compressed power is 1.18 kW, which corresponds to 1.18-mJ pulse energy.

Figure 3(a) shows the measured and transform-limited autocorrelation traces and spectrum of the compressed pulses at 1.18-mJ pulse energy. The red solid line represents the measured autocorrelation trace with a full-width at half-maximum (FWHM) of 396 fs. The pulse duration is estimated to be 270 fs assuming a hyperbolic-secant profile. The inset of Fig. 3(a) shows the spectrum of the pulses centered at 1032.7 nm with a spectral width of 8.6 nm. The black dotted line in Fig. 3(a) shows the autocorrelation trace of the transform-limited pulse calculated from the spectrum, and its duration is 232 fs. The red and blue lines in Fig. 3(b) represent the diameters of compressed pulses in the horizontal and vertical directions after propagating through a 150-mm lens, respectively. The beam quality factor (M^2) is 1.20×1.20, and the inset shows the far-field beam-profile with an ellipticity of 0.98.

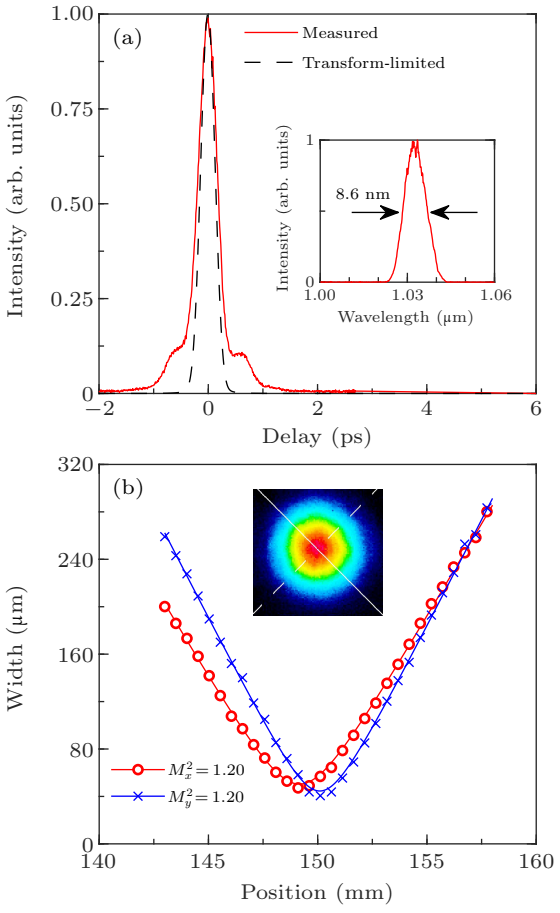


Fig. 3. (a) Autocorrelation traces and (b) beam quality of the compressed pulses at 1.18-mJ energy. Inset of (a): optical spectrum, inset of (b): beam profile.

Figure 4(a) shows the short-term average power change of combined pulses measured by another PD (not shown in

Fig. 1). The PD signal is filtered by a low-pass filter to isolate average power. The phase residual error calculated by the PD signal is about $\lambda/29.5$, which is typical for the SPGD method.[17] Figure 4(b) shows the average power of the compressed pulses measured at 1.12 kW by a water-cooled thermal power meter. Within 12 hours, the standard deviation is 3.6 W, indicating that the average-power instability (RMS) is 0.32%.

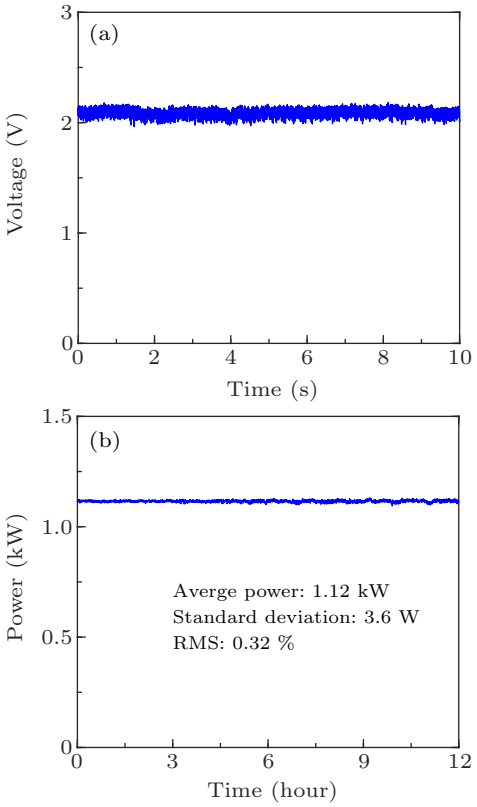


Fig. 4. (a) Short-term and (b) long-term power stability of the compressed pulses.

4. Conclusion and perspectives

We develop an eight-channel rod-type Yb-fiber CBC system with excellent power stability. The phase stabilization is based on the SPGD method, and the group-delay and beam-pointing control are realized on a novel multi-step hill-climbing method. To the best of our knowledge, we are the first to propose and implement this multi-step hill-climbing method for CBC. This CBC system delivers 1-MHz, 270-fs pulses with the average power up to 1.18 kW corresponding to 1.18-mJ pulse energy. Ongoing work is to further compress the pulses to a duration < 30 fs using a gas-filled multi-pass cavity.

The output power of each channel can be further increased to 300 W by increasing the input pulse power from 5 W to 30 W,[9] while the accumulated nonlinear phase can be reduced by increasing the dispersion of stretcher and compressor. The total output power of eight channels is expected to reach 2.4 kW, leading to a combined and compressed output power above 2 kW and a pulse energy above 2 mJ. In addition, we are planning to increase the channel number to sixteen. Together with the increase of input power, it is expected that the average power (pulse energy) can exceed 4 kW (4 mJ). The pulse energy can be further increased by time division techniques. In 2024, Rainville *et al.* achieved the combination of 81 temporal replicas using coherent pulse stacking amplification (CPSA), and generated 10-mJ pulse energy from a single fiber amplifier.[18] Combining with this CPSA technology, Yb-fiber CBC systems are able to produce multi-kW femtosecond pulses with sub-J level energy, which constitutes an enabling research tool for particle acceleration.

Acknowledgments

Project supported by the Key Deployment Special Research Project of the Chinese Academy of Sciences (Grant No. PTYQ2022YZ0001), the National Natural Science Foundation of China (Grant Nos. 62175255 and 62227822), and the National Key Research and Development Program of China (Grant No. 2021YFB3602602).

References

[1] Shirozhan M, Mondal S, Grósz T, *et al.* 2024 *Ultrafast Science* **4** 0067
[2] Teng H, Zhong S Y, He X K, Zhao K, Yun C X, Dong S and Wei Z Y 2024 *Acta Opt. Sin.* **44** 1732016 (in Chinese)
[3] Baker L R, DiMauro L F, Turro C, Gupta J A, Kawakami R K, Allison T K, Ronningen T J, Scarborough T D, Leshchenko V, Shields S S and Beetar J E 2025 *ACS Central Science* **11** 12
[4] Müller M, Aleshire C, Klenke A, Haddad E, Légaré F, Tünnermann A and Limpert J 2020 *Opt. Lett.* **45** 3083
[5] Stark H, Benner M, Buldt J, Klenke A and Limpert J 2023 *Opt. Lett.* **48** 3007
[6] Eidam T, Rothhardt J, Stutzki F, Jansen F, Hädrich S, Carstens H, Jauregui C, Limpert J and Tünnermann A 2011 *Opt. Express* **19** 255
[7] Jauregui C, Stihler C and Limpert J 2020 *Adv. Opt. Photon.* **12** 429
[8] Pedersen M E, Johansen M M, Olesen A S, Michieletto M, Gaponenko M and Maack M D 2022 *Opt. Lett.* **47** 5172
[9] Wang D L, Shi Z, Wang J S, Wu H Y, Zhang X H and Chang G Q 2024 *Acta Phys. Sin.* **73** 134204 (in Chinese)
[10] Shi Z, Chang H X, Wang D L, Guo H Y, Dong Z K, Du Z H, Liang C B, Li C, Zhou P, Wei Z Y and Chang G Q 2025 *Acta Phys. Sin.* **74** 014205 (in Chinese)
[11] Wang Z H, Peng S X, Xu H, Wang Y H, Li Z Y, Zhang Q B and Lu P X 2026 *Chinese Journal of Lasers* **53** 0201001 (in Chinese)
[12] Klenke A, Hädrich S, Eidam T, Rothhardt J, Kienel M, Demmler S, Gottschall T, Limpert J and Tünnermann A 2014 *Opt. Lett.* **39** 6875
[13] Shay T M, Benham V, Baker J T, Sanchez A D, Pilkington D and Lu C A 2017 *IEEE J. Sel. Top. Quantum Electron.* **13** 480
[14] Chang H X, Chang Q, Xi J C, Hou T Y, Su R T, Ma P F, Wu J, Li C, Jiang M, Ma Y X and Zhou P 2020 *Photonics Research* **8** 1943
[15] Weiss S B, Weber M E and Goodno G D 2012 *Opt. Lett.* **37** 455
[16] Goodno G D and Weiss S B 2012 *Opt. Express* **20** 14945
[17] Yu C X, Kansky J E, Shaw S E J, Murphy D V and Higgs C 2006 *Electron. Lett.* **42** 1024
[18] Rainville A, Whittlesey M, Pasquale C, Jing Y W, Chen M S, Pei H Z, Ruppe J, Du Q, Zhang Z G, Chang G Q, Kärtner F X and Galvanauskas A 2024 *Optica* **11** 1540